

Electric vehicle charging system model for accurate electricity system planning

ISSN 1751-8687

Received on 18th September 2017

Revised 5th July 2018

Accepted on 20th July 2018

E-First on 31st August 2018

doi: 10.1049/iet-gtd.2018.5580

www.ietdl.org

Arturs Purvins^{1,2} ✉, Catalin-Felix Covrig¹, Georgios Lempidis^{3,4}

¹European Commission, JRC – Directorate C Energy, Transport and Climate, Postbus 2, 1755 ZG Petten, The Netherlands

²European Distributed Energy Resources Laboratories (DERlab) e.V., c/o Fraunhofer IEE, Koenigstor 59, 34119 Kassel, Germany

³Valeo Siemens eAutomotive Germany GmbH, Frauenaucher Str. 85, 91056 Erlangen, Germany

⁴Fraunhofer IEE, Institute for Energy Economics and Energy System Technology, Koenigstor 59, 34119 Kassel, Germany

✉ E-mail: arturs.purvins@ec.europa.eu

Abstract: This article presents a novel electric vehicle (EV) charging system model. The model introduces power constraints in the grid-to-battery converter to improve modelling accuracy. Simulation results of the presented model indicate EV charging impact on a low-voltage electricity grid. Even though most of the battery charging load is spread evenly during desired times (e.g. off-peak load during night), power constraints of the EV model result in narrow peak loads. Plug-in EVs bring additional load to the electricity grid. If not managed properly, high EV deployment may lead to unnecessary grid investments due to high-peak currents of EV charging. Rising numbers of grid connected EVs is a challenging task in the future electricity grid planning. Thus an accurate EV charging system model is essential for reliable analysis of EV deployment.

1 Introduction

This study aims (i) to develop and to test an accurate simulation model for an EV charging system and (ii) to identify electricity grid challenges and opportunities at high EV deployment.

In most of the available literature, electric vehicle (EV) charging systems are modelled as completely flexible loads (generators) where the EV load scheduling is managed to avoid grid congestions and lower the EV charging cost. For instance, in the study of Hu *et al.* [1], the only constraints on the EV charging system are the battery capacity and the rated power of the charging converter. Wang *et al.* [2] developed a comprehensive EV charger model where power electronics are modelled in detail. Other constraints besides the rated power of the converter are not applied. Recent studies present detailed models for electrochemical cell battery simulation: The battery system management model by Purvins and Sumner [3] takes into account battery ageing. This is already sufficient for general feasibility studies of battery systems. A review on various battery models for EV applications is offered by Fotouhi *et al.* [4]. Other EV-related studies investigate the potential net present revenues of potential vehicle-to-grid services (i.e. see study by Zhao *et al.* [5]). Madina *et al.* [6] studied EV charging infrastructure business models; they have reported that users who have access to private home charging are expected to be the early adopters of EVs. He *et al.* [7] searched for optimal locations for public EV charging points. Adepetu *et al.* [8] focused on EV policy trends and presented an EV model to study how different policies and battery technologies affect EV adoption.

All the aforementioned studies cover important topics on EV integration in the electricity system; however, without power converter constraints in the battery charging system, missing the real EV impact on power flows in electricity grid is highly possible.

A novel EV charging system model is developed for grid-connected EVs to improve accuracy in EV modelling. The proposed model considers constraints of the power converter which connects battery to electricity grid. These constraints limit minimum and maximum operation power of the converter at various state-of-charge (SoC) levels of battery. This is a unique property of the presented EV system model, which offers more accurate grid connected EV system modelling. It is known that

grid-connected EV is a relatively large load, and it needs to be modelled properly to achieve reliable results.

The proposed EV charging system model is tested under two case studies: (i) a low-voltage distribution feeder with ten residential buildings having two 24 kWh battery EVs each; (ii) a commercial site with four 4.4 kWh battery EVs.

An energy management methodology applied for the presented EV model was developed in the FP7 project EEPOS (Energy management and decision support systems for Energy POSitive neighbourhoods, <http://eepos-project.eu/>, [9]).

2 EV charging system model

The proposed EV charging system model is developed for a technical simulation of a battery charging/discharging operation. The input interfaces of the EV model are as follows:

- i. battery capacity;
- ii. battery availability (connection to the grid);
- iii. energy consumption while driving;
- iv. minimum SoC at departure;
- v. desired SoC at departure;
- vi. battery charging efficiency;
- vii. battery discharging efficiency;
- viii. rated power of the power converter;
- ix. power converter charging efficiency;
- x. power converter discharging efficiency;
- xi. power constraints as a function of the SoC.

The latter is power limits of the power converter which connects battery to electricity grid. These power constraints shown in Figs. 1 and 2 are assumptions made by authors to reflect a general behaviour of an EV charging. SoC is expressed in per unit values: SoC=0 indicates that battery is empty and cannot be further discharged. When the battery is fully charged, the SoC is 1. Power is expressed in % from the rated power of the power converter.

At low SoC of the battery the power converter cannot reach its rated power due to low voltage on the battery. Power flow (P)

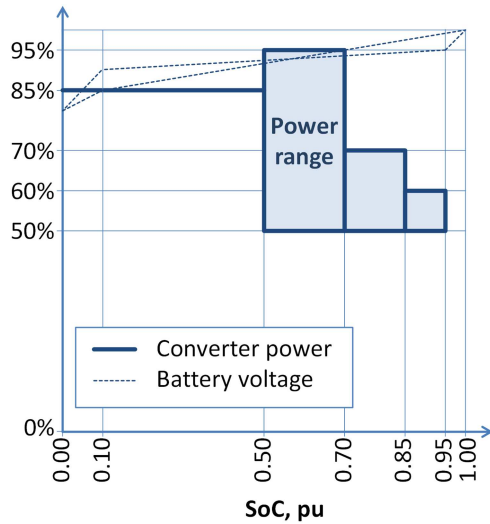


Fig. 1 Power converter constraints as a function of SoC: charging mode

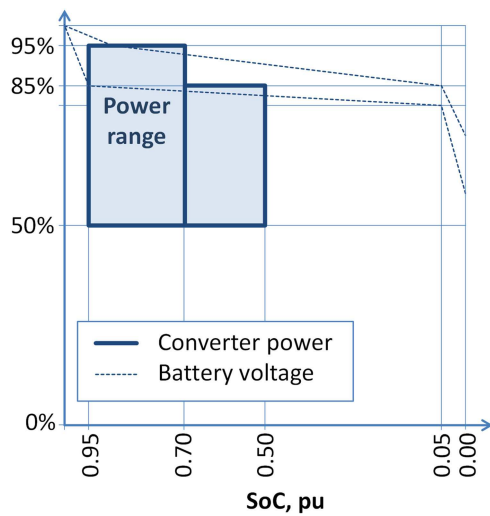


Fig. 2 Power converter constraints as a function of SoC: discharging mode

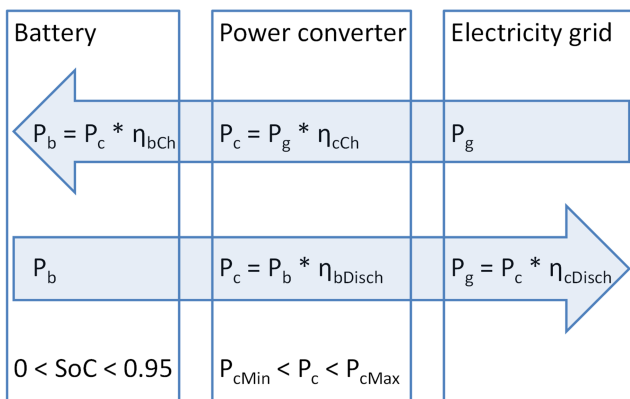


Fig. 3 Battery-to-grid power flows

between the converter and the battery is a result of a multiplication of the battery-to-converter current (I) and the battery voltage (V): $P = IV$. The battery voltage (V) varies depending on the SoC. The maximum value of the current (I) is limited by the current rating in the power switches in the converter. It is constant. At constant current (I) the maximum battery-to-converter power flow (P) is proportional to the battery voltage (V). Battery voltage drops at low SoC and so does the maximum converter power.

Figs. 1 and 2 show this relation depicting voltage range of some lithium-ion [10, 11] and Nickel-metal hydride [12] batteries. 100%

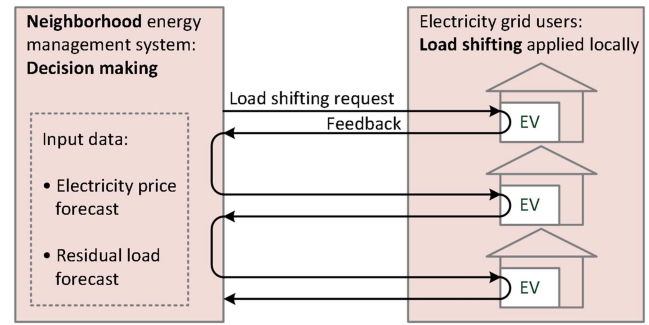


Fig. 4 Energy management concept

represents voltage of a fully charged battery. Maximum converter power constraint follows battery voltage pattern.

During charging mode at battery SoC < 0.5 , the power converter can reach only 85% of its rated power (Fig. 1) due to low battery voltage. 0.5 SoC in this study is considered the minimum SoC of the battery, which should be reached as soon as possible when EV is connected to the grid, i.e. the converter operates at maximum power until the battery is half charged. At battery SoC above the minimum (0.5) the operation range of the power converter is set by the minimum and maximum power. This flexibility can be used in energy management systems to adapt battery charging/discharging power to the needs of the electricity grid. The upper power limit at higher battery SoC between 0.5 and 0.7 rises to 95%, while the minimum power is set to 50% of the converter rated power. The lower limit is required to keep converter operation in a range where the converter efficiency is relatively high. Further constraints in upper power at higher SoC are introduced due to the necessity of keeping charging currents low for the prevention of overcharge. Battery charging stops at a SoC of 0.95. Similarly, at battery discharging, converter limits are set with minimum and maximum powers as shown in Fig. 2. Note that for each particular case the model should be calibrated accordingly for reliable results.

When connected to electricity grid, EV battery can be charged or discharged. Power exchange between the EV charging system and grid is depicted in Fig. 3. During charging, power from grid (P_g) flows through converter to the battery. Power received by the battery (P_b) is slightly reduced due to power conversion losses in the converter (η_{cCh}) and the battery (η_{bCh}). Similarly losses occur while discharging. SoC of the battery is maintained from 0 to 0.95; and operating power range of the power converter (from P_{cMin} to P_{cMax}) depends on the SoC.

3 Energy management

The proposed simulation model of the EV charging system applies for any energy storage system with a secondary electro-chemical battery. The management concept of the EV charging system is illustrated in Fig. 4. The decision on the optimal energy management is taken centrally on the neighbourhood level following the methodology of Purvins and L'Abbate [9]. The neighbourhood could consist of all grid users on the low-voltage side of the distribution grid substation. The neighbourhood management system sends a load shifting request to the buildings hosting EVs. The EV charging system manages the charging–discharging of the EV battery following the load shifting request. The EV charging system can detect when the vehicle is connected to the grid, but does not know the leave time.

The load shifting request is calculated based on the following energy management aims:

- local consumption of distributed generation;
- cost efficient energy management (price following);
- peak load shaving.

The load shifting request is a data array of the following integers: $-2, -1, 1, 2$, where each number is linked to a specific time period for the next 24 h. Description of the load shifting request numbers is detailed in Table 1. In general, negative

numbers indicate times from which load is suggested to be shifted, and positive numbers – times to which load is suggested to be shifted. For example, negative signal suggests supplying EV battery power to grid, and positive signal suggest battery charging. During times of ‘-2’ and ‘2’ load shifting is highly suggested. The input data for the calculation of the load shifting request profile is (i) electricity price and (ii) residual load (see Table 1). The latter is load minus generation.

For example, if the daily peak load is 10 kW, case #1 will apply at a high price and a load above 7.5 kW. The residual load criteria for cases #4 and #5 differ from the criteria presented by Purvins and L'Abbate [9]. These have been changed to prevent the creation of narrow peak loads at battery charging, since EV is quite a big load, compared with other electrical loads in residential buildings.

The neighbourhood energy management system calculates the load shifting request for an individual building. The buildings receive the request one after another as seen in Fig. 4. Firstly, the load shifting request is calculated for one building. Then this building provides feedback to the neighbourhood energy management system regarding the planned load shifting. After receiving the feedback, the neighbourhood energy management

system calculates the load shifting request for another building, taking into account the planned load shifting of the first building. The rest of the buildings are addressed in the same way. Such distribution of the load shifting requests is initiated every time when the neighbourhood energy management system receives updates on the energy state in the neighbourhood, like the weather forecast update.

The operation methodology of the EV charging system model is presented in Fig. 5. The algorithm in Fig. 5 applies for time periods when battery is connected to the grid. The algorithm is initiated whenever an updated load shifting request (from the neighbourhood energy management system) is received by the EV model. The first part of the algorithm is battery charging planning. If the battery SoC is below SoC_min, battery is charged to SoC_min with full power during times with load shifting request values of 1 and 2, if possible. SoC_min = 0.5 is the minimum SoC of the battery which should be reached by the EV model as soon as possible.

The next step is to charge the battery to SoC_max during times when the load shifting request is 2, if possible. SoC_max = 0.95 is the maximum SoC of the battery at which the battery charging is

Table 1 Decision table for the load shifting request

Case no.	Price	Residual load	Signal	Action
1	high	above 75% of peak load	-2	shift load <i>from</i> these times: Strongly suggested
2	high	positive and below 75% of peak load	-1	shift load <i>from</i> these times
3	high	negative	+2	shift load <i>to</i> these times: strongly suggested
4	low	above 50% of peak load	+1	shift load <i>to</i> these times
5	low	below 50% of peak load	+2	shift load <i>to</i> these times: Strongly suggested

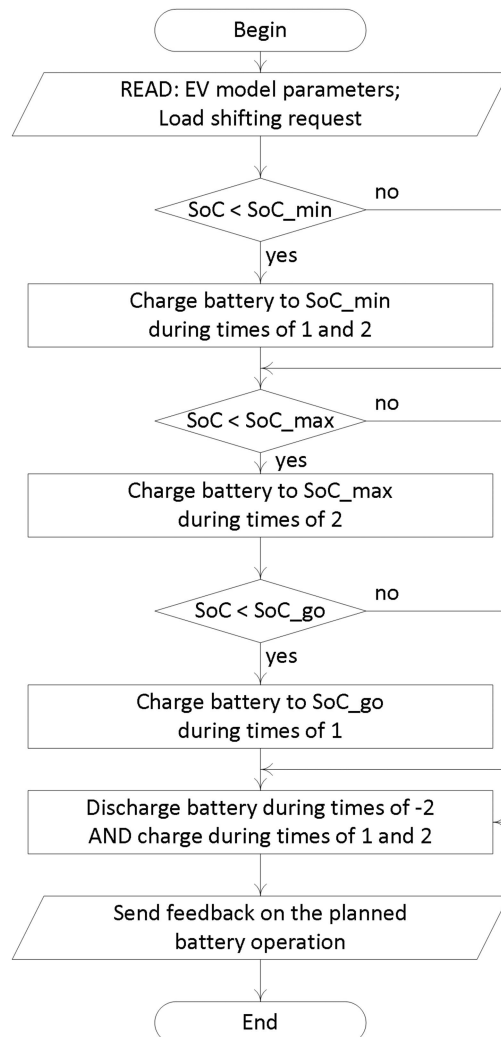


Fig. 5 EV model operation planning following the load shifting request values (from -2 to 2)

stopped. If possible, after these steps, if the battery SoC is still below SoC_{go} (0.8), the battery is charged to SoC_{go} during the times of the load shifting request value of 1. Finally, the battery is discharged during times when the load shifting request is -2 . This discharge can be compensated with additional charging during times 1 and 2.

All the planning steps of the algorithm should be in line with the EV model parameters, including the power constraints (Figs. 1 and 2). The outcome of the algorithm is a planned battery operation pattern for the next 24 h. This operation pattern is applied to the EV model and is sent to the neighbourhood energy management system for further energy planning.

4 EV test cases

4.1 Residential feeder

Twenty EVs with a 24 kWh battery each are distributed evenly along a residential feeder with ten buildings, i.e. two EVs per building. Each building has a charging point for two EVs. The feeder is depicted in Fig. 6. Buildings are represented as grid nodes with PV systems and loads. Loads refer to electrical loads in buildings including EVs.

Feeder topology and main parameters are obtained from the study of Papaioannou *et al.* [13]. The parameters are adapted to meet the load and have the following properties:

- Three phase, with line-to-line voltage of 400 V.
- Three single-phase PVC insulated cables with copper conductors. Each conductor has a section area of 70 mm², an AC resistance of 0.321 Ω /km at 70°C and a reactance of 0.107 Ω /km at 50 Hz.
- Neutral cable of the same type: conductor section area of 16 mm², AC resistance of 1.38 Ω /km at 70°C, reactance of 0.078 Ω /km at 50 Hz.
- A distance of 60 m between neighbouring nodes.
- Active-inductive load with $\cos \phi = 0.8$. The EV is considered as an active load.

Load and PV generation profile used in the sensitivity analysis are the same as in the study by Purvins and L'Abbate [9]. This is a 5-day profile with a time step of 10 min as shown in Fig. 7. Load data is obtained from the EEPOS project field test measurements in June in Langenfeld (Germany). It is an average daily load profile from three apartments – each with two inhabitants, measured under a single electricity tariff. The average daily consumption is 4.54

kWh per apartment. It is assumed that each building (load 1–10 in Fig. 6) comprises of six apartments with such profile.

The PV generation profile comprises 5-day historical data of 1.92 kWp (panel output) PV plant measured in June. The PV power plant is located in Kassel (Germany), on the Fraunhofer IWES premises. In order to simulate a slight PV generation surplus, the PV plant size is scaled up ten times (see Fig. 7).

The time periods of two-tariff electricity price profile are adapted from some energy retailers in Germany. The low price is found during the night, from 22:00 to 6:00.

The parameters of the modelled EV charging systems are listed in Table 2. EV1 and EV2 systems are applied for each building in the residential feeder. As can be seen in Table 2, EV1 and EV2 have different driving patterns. This also leads to difference in the consumed energy while driving. The driving patterns are taken from previous EV studies [14–16]. The first vehicle, EV1, is away from 7:00 and returns home at 17:00. The second vehicle, EV2, leaves the house for 3 h: from 10:00 to 13:00.

Buildings in the distribution feeder are approached individually by the neighbourhood energy management system as illustrated in Fig. 4.

4.2 Commercial site

Four EVs with 4.4 kWh battery each have charging stations connected to the grid node of a commercial site. Commercial load and PV generation profiles obtained from the Joint Research Centre (European Commission) site in Petten [17] are depicted in Fig. 8. The load represents of 1 week at the beginning of June. In order to visualise the effects of the EVs, the load and PV profiles are downscaled. The shape of the profiles remains the same. The proportion of the commercial load and PV kept so that PV generation is close to the peak load rise during a day.

Dual pricing is not applied in this test case. Price is assumed 'low' in the simulation. As a result Case 4 in Table 1 applies for every time step due to low price and load above 50% of the peak load. In order to distribute the EV load evenly during charging hours, in cases 4 and 5 (Table 1) a rise of the load threshold is introduced (50% is changed to 80%).

The parameters of the EV charging system are listed in Table 2. EV3–6 are applied for this case. Additional model input parameters are presented in Table 3: time periods when EVs are connected to the grid and battery SoC at the beginning of the grid connection. When two time periods are listed in 1 day for the same vehicle, two SoC values are given: the first SoC value (as listed in the table) refers to the first time period, and the second value – to the second.

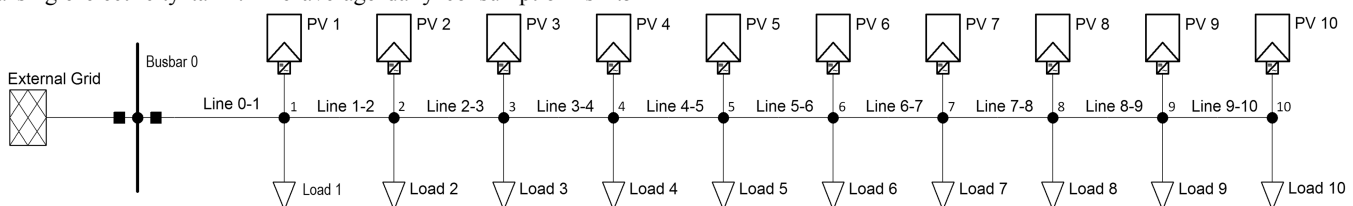


Fig. 6 Residential feeder with ten buildings represented as PV systems and loads

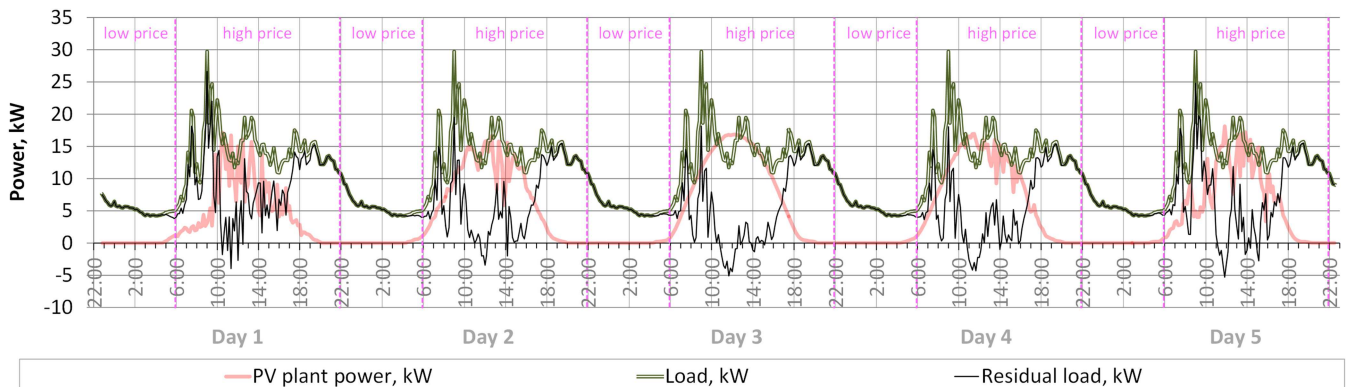


Fig. 7 Load, PV generation, residual load: residential feeder

It can be seen in Table 3 that the EVs are connected to the grid during working hours. These could be vehicles of employers commuting to work.

In this test case each vehicle charging system is addressed separately by the neighbourhood energy management system (depicted Fig. 4), i.e. EV systems are approached one after another. Battery discharging is not applied since EVs are parked in the commercial site (and connected to the grid) during peak load hours.

5 Results

5.1 Residential feeder

Results of EV impact on the residential feeder are shown in Fig. 9. An EV is a relatively big load. It can change the entire load profile. EVs are charged during the night at low electricity price. As explained previously (in Section 3), each building in the test feeder receives its own unique load shifting profile, which contains information on optimal battery charging–discharging times.

Firstly, the load shifting request profile is sent to the first building (e.g. in Node 1, Fig. 6). This request for a time period from 12:00 in day 1 to 12:00 in day 2 is depicted in Fig. 9. It was calculated taking into account the residual load profile in the feeder

and the electricity price. Value ‘2’ in the load shifting request indicates highly suggested charging times, and ‘–2’ – times when it is highly suggested to supply energy to the grid.

The addressed building has two EVs: EV1 and EV2. These EVs are planning their battery utilisation patterns based on the load shifting request. Fig. 9 shows the charging pattern of EV1 (on the top of the residual load) with dotted line: from 12:00 in day 1 to 12:00 in day 2. EV1 is charged during the night at low electricity price for 2 h: from 22:20 to 01:20. The power drawn from the grid by EV1 is close to 6 kW. In total, EV1 consumes 11.5 kWh from the grid. This amount of energy comprises EV battery charging to SoC = 0.95 and energy losses in the EV charging system. Between 19:00 and 20:00, battery supplies energy to the grid for 20 min. This is the only time period of ‘–2’ when EV1 is connected to the grid and falls under Case #1 at the time of calculation: peak load and high price (see Table 1).

The load profile that resulted with two EVs per building is presented in Fig. 9. From 22:00 to 6:00, the EVs charging creates wide base-load with narrow peaks on the top. These peaks occur due to power constraints of the EV model (Table 2), mainly because of minimum operation power of the power converter. EV charging peaks exceed the morning peak load.

Table 2 EV charging system model parameters

Parameter	EV1	EV2	EV3–6
battery capacity, kWh	24	24	4.4
battery connected to the grid, time	17:00–7:00	10:00–13:00	variable
energy consumption while driving, kWh	5	2	variable
minimum SoC when leaving (SoC _{go}), p.u.	0.5	0.5	0.5
desired SoC when leaving (SoC _{go}), p.u.	0.8	0.8	0.8
battery charging efficiency, %	97.5	97.5	97.5
battery discharging efficiency, %	97.5	97.5	97.5
rated power of the power converter, kW	10	10	2.2
power converter charging efficiency, %	95	95	95
power converter discharging efficiency, %	95	95	95

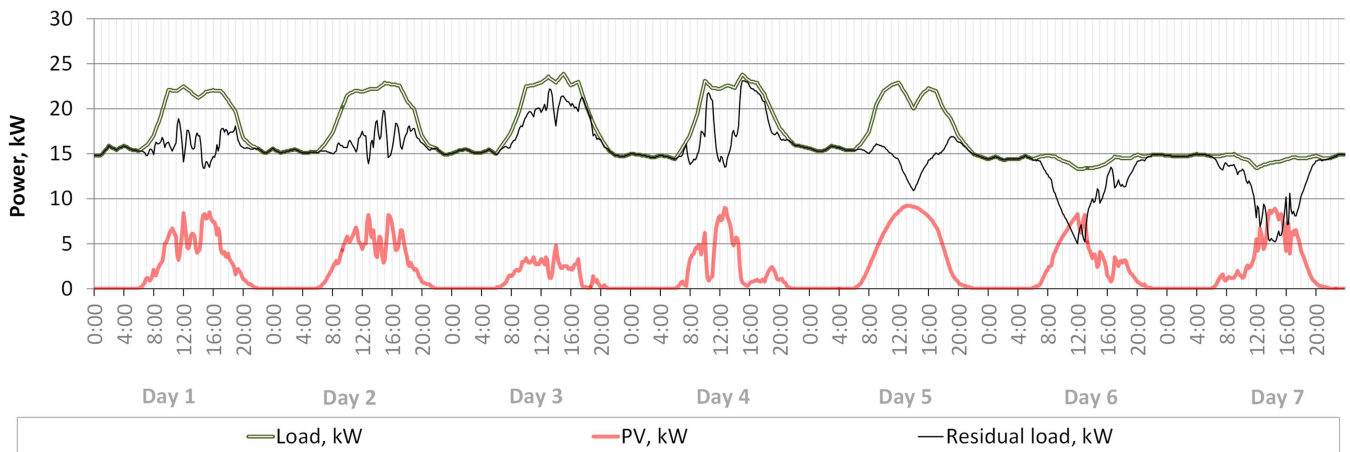


Fig. 8 Load, PV generation and residual load: commercial site

Table 3 Extra EV model parameters: commercial site

Day	Parameter	EV3	EV4	EV5	EV6
1	parking time	8:15–10:10; 11:35–17:10	8:37–17:09	8:25–17:01	8:25–12:10; 13:08–17:11
1	SoC, p.u.	0; 0.43	0	0	0; 0.78
2	parking time	8:25–16:16	8:27–17:23	8:11–17:18	8:16–15:37
2	SoC, p.u.	0	0	0	0
3	parking time	8:18–17:18	8:23–17:33	8:26–17:30	8:11–12:09; 13:42–17:13
3	SoC, p.u.	0	0	0	0; 0.88
4	parking time	8:05–17:14	8:25–17:15	7:55–17:26	8:35–17:10
4	SoC, p.u.	0	0	0	0
5	parking time	8:56–16:01	8:14–15:48	8:15–12:16; 13:18–17:06	9:15–17:01
5	SoC, p.u.	0	0	0; 0.89	0

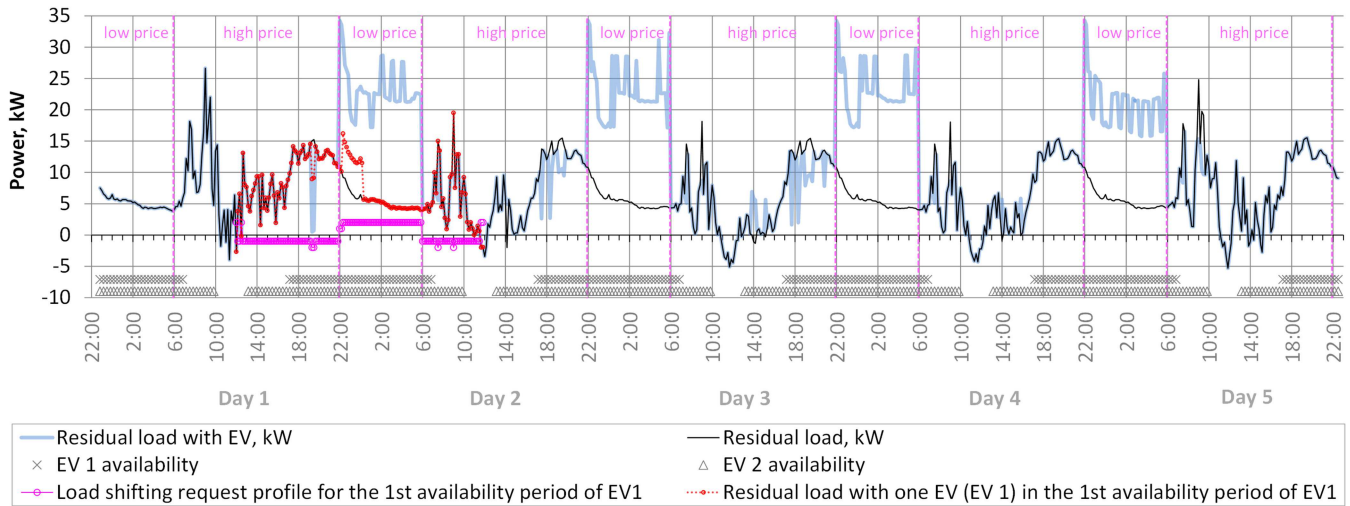


Fig. 9 Residual load without and with EVs and EV availability: residential feeder

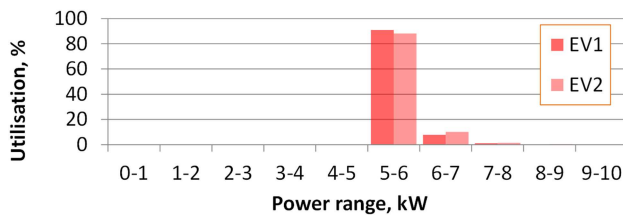


Fig. 10 Utilisation of power converter (grid to battery) loading: residential feeder

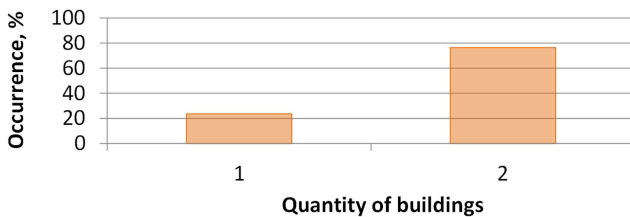


Fig. 11 Number of buildings with simultaneous charging of EVs

EV contributes in peak load shaving between 19:00 and 20:00 as seen in Fig. 9. The usefulness of such a load reduction should be further examined, because in the subject feeder it does not really contribute in the peak load shaving. Moreover, electricity cost saving incentive for power flows from battery to grid may not be attractive. At two-tariff pricing as currently practiced by energy service providers in Germany – 0.30 and 0.25 EUR/kWh for high and low price, respectively – average daily saving per EV is 1 euro cent.

Generation surplus compensation cannot rely on EV. In a sunny day at noon EV may not be available for PV power storage.

Generation surplus causes voltage rise in the feeder, whereas, high load leads to voltage drop. Additional results in load flow parameters in the feeder are obtained with PowerFactory (DIgSILENT). A maximum voltage of 231 V appears during times of PV generation surplus. Minimum voltage depends on the peak load value. EVs charging peaks during the night lead voltage drops to 221 V. Extra load also brings additional electricity distribution losses in the feeder. In the subject feeder, the average active losses per day rise from 14 kWh (without EVs) to 27 kWh (with EVs).

EV as a flexible (active) load could also participate in the grid voltage control. From the voltage perspective, Papaioannou *et al.* examine the optimal topology of flexible load along the feeder [18] and present methodology to calculate maximum generation/load capacity that can be installed in a radial LV feeder at a fixed point [19]. In general, peak load shaving and voltage control are related grid services since lower peak loads will reduce possible voltage drop.

Furthermore, utilisation of power converter loading in charging operation is depicted in Fig. 10. As seen in Fig. 10, the charging

power never falls under 5 kW, which is the minimum operation power. High operation powers are not observed for both EVs (EV1 and EV2). This is result of relatively low battery use while driving (see energy consumption while driving in Table 2). In most of the cases, the charging power is between 5 and 6 kW. Only 10% of the charging time the charging power is between 6 and 7 kW.

Another outcome of this study case is EV charging distribution during charging hours. Fig. 11 shows results on maximum number of buildings with simultaneous EV charging. It can be seen that in the most of cases (76%) EVs are charged simultaneously in two buildings, and in the rest of time – only in one building. This indicates well-managed EV charging, i.e. EVs are charged in different times preventing creation of peak load. Information in Fig. 11 can be used while examining grid support services, such as phase balance. The three-phase power converter can shift active load from one phase to another in such a way that it contributes to power balance (among phases) when necessary.

5.2 Commercial site

Results of EV impact on commercial load profile are presented in Fig. 12. It can be seen that EVs create a peak load in the morning at the times when just connected to the grid. This is due to fact that in the morning on arrival at the commercial site, the battery is always empty (see Table 3) and it needs to be charged to the SoC = 0.5 as soon as possible. Further charge of battery is distributed more evenly during the day. In Day 5, battery charging is applied between 12:00 and 16:30. During this time, EVs are balancing off-peak load created by high PV generation.

Occurrence frequency of various loading ranges of the power converter (connecting battery to grid) is depicted in Fig. 13. As in the morning hours, EVs are connected with empty batteries to the grid, the loading of the converter varies widely from 50% to full load operation.

6 Conclusions

The presented EV charging system model introduces constraints in the power converter which connects battery to electricity grid. These constraints limit minimum and maximum operation power of the converter at various SoC levels of battery. It is a new feature in EV modelling exercises, which increases modelling accuracy.

Power exchange between the EV charging system model and electricity grid is managed following methodology of Purvins *et al.* [9]. EV battery charging is distributed well in two test cases; however, narrow charging peaks appear frequently due to constraints (i) in the power converter and also (ii) in the energy management. The latter is the minimum SoC of the battery (50%) which should be reached as soon as possible.

Further research includes configuring the EV charging system model to match dynamic characteristics of a battery-to-grid system in the Smart Grids Interoperability Laboratory of the Joint

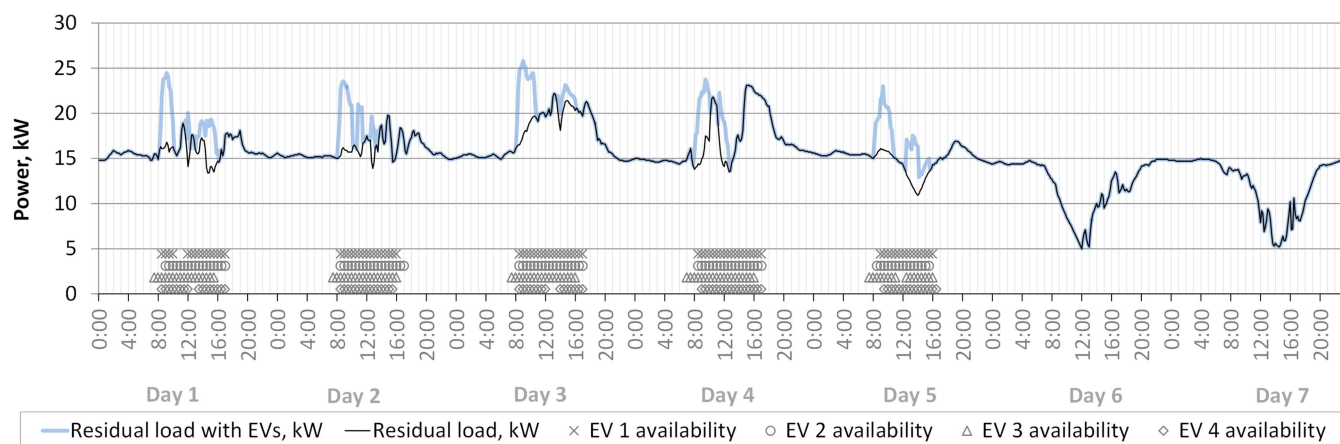


Fig. 12 Load (without and with EVs) and EV availability: commercial site

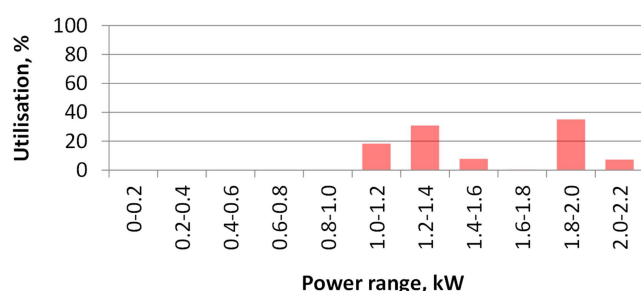


Fig. 13 Utilisation of power converter (grid to battery) loading: commercial site

Research Centre [20]. Comparison between modelling results and laboratory measurements will show how well peak loads can be captured with the proposed EV model.

7 Acknowledgment

The work presented here has been partially carried out in the frame of the EEPOS project, which has received co-funding from the European Union's Seventh Programme for research, technological development and demonstration (grant no. 600050).

8 References

- [1] Hu, J., Morais, H., Lind, M., *et al.*: 'Multi-agent based modeling for electric vehicle integration in a distribution network operation', *Electr. Power Syst. Res.*, 2016, **136**, pp. 341–351, doi: 10.1016/j.epsr.2016.03.014
- [2] Wang, M., Mu, Y., Jia, H., *et al.*: 'Active power regulation for large-scale wind farms through an efficient power plant model of electric vehicles', *Appl. Energy*, 2017, **185**, (2), pp. 1673–1683, doi: 10.1016/j.apenergy.2016.02.008
- [3] Purvins, A., Sumner, M.: 'Optimal management of stationary lithium-ion battery system in electricity distribution grids', *J. Power Sources*, 2013, **242**, pp. 742–755, doi: 10.1016/j.jpowsour.2013.05.097
- [4] Fotouhi, A., Auger, D. J., Propp, K., *et al.*: 'A review on electric vehicle battery modelling: from lithium-ion toward lithium-sulphur', *Renew. Sust. Energy Rev.*, 2016, **56**, pp. 1008–1021, doi: 10.1016/j.rser.2015.12.009
- [5] Zhao, Y., Noori, M., Tatari, O.: 'Vehicle to grid regulation services of electric delivery trucks: economic and environmental benefit analysis', *Appl. Energy*, 2016, **170**, pp. 161–175, doi: 10.1016/j.apenergy.2016.02.097
- [6] Madina, C., Zamora, I., Zabala, E.: 'Methodology for assessing electric vehicle charging infrastructure business models', *Energy. Policy.*, 2016, **89**, pp. 284–293, doi: 10.1016/j.enpol.2015.12.007
- [7] He, S.Y., Kuo, Y.-H., Wu, D.: 'Incorporating institutional and spatial factors in the selection of the optimal locations of public electric vehicle charging facilities: a case study of Beijing, China', *Transp. Res. C, Emerg. Technol.*, 2016, **67**, pp. 131–148, doi: 10.1016/j.trc.2016.02.003
- [8] Adepetu, A., Keshav, S., Arya, V.: 'An agent-based electric vehicle ecosystem model: San Francisco case study', *Transp. Policy*, 2016, **46**, pp. 109–122, doi: 10.1016/j.tranpol.2015.11.012
- [9] Purvins, A., L'Abbate, A.: 'Automated energy management in distributed electricity systems: an EEPOS approach', *Int. J. Green Energy*, 2017, **14**, (12), pp. 1034–1047, doi: 10.1080/15435075.2017.1355309
- [10] Cui, X., Shen, W., Zhang, Y., *et al.*: 'A novel active online state of charge based balancing approach for lithium-ion battery packs during fast charging process in electric vehicles', *Energies*, 2017, **10**, (11), p. 1766, doi: 10.3390/en10111766
- [11] Richtek Technology: 'Designing applications with Li-ion batteries'. Available at: <https://www.richtek.com/battery-management/en/designing-li-ion.html>, accessed July 2018
- [12] Storage Battery Systems: 'Small rechargeable battery cells & packs'. Available at: <https://www.sbsbattery.com/products-services/by-product/batteries/small-rechargeable-sealed-lead-acid-battery-cells-packs.html>, accessed July 2018
- [13] Papaioannou, I.T., Purvins, A., Demoulias, C.S.: 'Reactive power consumption in photovoltaic inverters: a novel configuration for voltage regulation in low-voltage radial feeders with no need for central control', *Prog. Photovolt., Res. Appl.*, 2015, **23**, (5), pp. 611–619
- [14] Jian, L., Xue, H., Xu, G., *et al.*: 'Regulated charging of plug-in hybrid electric vehicles for minimizing load variance in household smart microgrid', *IEEE Trans. Ind. Electron.*, 2013, **60**, (8), pp. 3218–3226, doi: 10.1109/TIE.2012.2198037
- [15] Sanchez-Martin, P., Sanchez, G., Morales-Espana, G.: 'Direct load control decision model for aggregated EV charging points', *IEEE Trans. Power Syst.*, 2012, **27**, (3), pp. 1577–1584, doi: 10.1109/TPWRS.2011.2180546
- [16] Yoshimi, K., Osawa, M., Yamashita, D., *et al.*: 'Practical storage and utilization of household photovoltaic energy by electric vehicle battery'. Proc. IEEE PES Innovative Smart Grid Technologies (ISGT), Washington, DC, USA, January 16–20, 2012, doi: 10.1109/ISGT.2012.6175688
- [17] Vandenbergh, M.: 'Solar photovoltaic production at JRC Petten'. Available at <https://ses.jrc.ec.europa.eu/publications/reports/solar-photovoltaic-production-jrc-petten-%E2%80%93-monitoring-report>, accessed July 2018
- [18] Papaioannou, I.T., Purvins, A., Tzimas, E.: 'Demand shifting analysis at high penetration of distributed generation in low voltage grids', *Electr. Power Energy Syst.*, 2013, **44**, (1), pp. 540–546, doi: 10.1016/j.ijepes.2012.07.054
- [19] Papaioannou, I.T., Purvins, A.: 'A methodology to calculate maximum generation capacity in low voltage distribution feeders', *Electr. Power Energy Syst.*, 2014, **57**, pp. 141–147, doi: 10.1016/j.ijepes.2013.11.047
- [20] JRC, Smart Grids Interoperability Laboratory: Available at <https://ec.europa.eu/jrc/en/research-facility/european-interoperability-centre-electric-vehicles-and-smart-grids>, accessed July 2018